Pyrolysis of Paper Sludge and Utilization for Ionic Dye Adsorption

Shao-Hua Hu,[a,*] and Shen-Chih Hu [b]

Paper sludge was pyrolyzed to synthesize an adsorbent for ionic dyes. Two reagents, Methylene Blue (MB) and Procion Red MX-5B (PR), were chosen as adsorbates. Pyrolysis of paper sludge was conducted at 600°C for 1 h under a nitrogen atmosphere, and the carbonized sample was washed with 1 M HCl for 30 min to remove inorganic salts (such as calcium) and to increase the carbon content. Scanning electron microscope (SEM) imaging showed that the particle size of the pyrolyzed paper sludge was obviously reduced when the acid-washing process was applied. Additionally, the specific surface area had increased from 13.25 to 193.86 m^2/g. The isoelectric point was around pH 3, which meant the adsorbent revealed positive charge to adsorb anionic dye (PR) when pH was below 3. On the other hand, cationic dye (MB) was adsorbed well under high pH values because of the negative surface charge of the adsorbent. The Langmuir equation was adopted to determine maximum absorption capacity. For MB and PR, the maximum absorption capacities were 119.05 mg/g and 65.79 mg/g, respectively. The adsorption kinetic study revealed that MB and PR adsorptions fit the pseudo-second-order kinetic model well. The activation energies for MB and PR were 12.32 kJ/mol and 2.88 kJ/mol, respectively. The results presented indicate that paper sludge can be pyrolyzed to form a dye adsorbent for cationic and anionic dyes.

Keywords: Paper sludge; dye adsorption; pyrolysis; Methylene Blue; Procion Red

*Contact information: a: Dept. of Environmental Resources Management, Dahan Institute of Technology, Hualian, Taiwan; b: Dept. of Material Science and Engineering, National Dong Hwa University, Hualian, Taiwan; *Corresponding author: shaohwa@ms01.dahan.edu.tw*

INTRODUCTION

Dyes can be used in many industries, such as in food, paper, textile, rubber, and plastics, in order to color products (Crini 2006; Olivella *et al.* 2012). After manufacturing, dyes are washed and dissolved in the wastewater. Dyes in wastewater are difficult to remove when utilizing conventional wastewater treatment methods. Dye molecules consist of two key components: 1) chromophores, which are responsible for producing color; and 2) auxochromes, which augment the chromophores, render the dye soluble in water, and enhance dye adsorption affinity toward the substrate (Gupta and Suhas 2009). Dyes are, by design, recalcitrant organic molecules that are stable when exposed to light, heat, and oxidizing agents (Sun and Yang 2003). Methods of dye removal from wastewater include coagulation, filtration, advanced oxidation processes, electrochemical methods, and adsorption (Gupta and Suhas 2009). Shi *et al.* (2007a) studied the removal of Direct Black 19, Direct Red 28, and Direct Blue 86 by coagulation with three different Al-based coagulants. A synthesized coagulant, designated as Al_{13}, was produced following the method of Shi *et al.* (2007b), and compared with $AlCl_3$ and polyaluminum

chloride (PAC), a traditional Al-based coagulant. The results showed that the coagulation of direct dyes could be greatly affected by pH, and the coagulation efficiency order was Al_{13} > polyaluminum chloride > $AlCl_3$. Kim *et al.* (2005) combined nano-filtration (NF) and reverse osmosis (RO) membranes to investigate the operating conditions for Reactive Yellow 145 (RY145) and Reactive Black 5 (RB5) removal. By combining NF and RO membranes, removal of chemical oxygen demand (COD) and of color were 98.4% and 99.6%, and the rejection efficiencies were 53.2% for RB5 and 96.6% for RY145. When compared to only NF membrane filtration, the removal of COD and of color were more than 96%, while the rejection efficiencies were 21.2% and 51.7% for RB5 and RY145, respectively. Lucas and Peres (2006) investigated the oxidative decolorization efficiency of RB5 in aqueous solution with Fenton and photo-Fenton processes. The optimal ratio of $[H_2O_2]$/[RB5] and $[H_2O_2]/[Fe^{2+}]$ were 4.9:1 and 9.6:1 at pH 3. The oxidative decolorizations of RB5 with Fenton and photo-Fenton processes were 97.5% and 98.1%, respectively, under optimal conditions. Total organic carbon (TOC) removal was 46.4% under the photo-Fenton process, which was higher than that of Fenton process (21.6%); the result indicates that a UV lamp has little effect on dye decolorization but is important in the reduction of TOC in dye solutions. Doğan and Türkdemir (2005) used an electro-chemical alternating treatment process of textile wastewater. The experiment was conducted using a batch-type divided electrolytic cell under constant potential with a Pt cage as anode and a Pt foil as cathode. The results showed that acidic conditions were more efficient for electrolysis. The electrolysis process achieved almost 100% color removal and 60% reduction in COD for a 0.1% (w/v) dye solution concentration at a pH 1 and with a 0.24 M of NaCl as an electrolyte for a 90 min treatment period.

Among the techniques mentioned, coagulation is a simple and economically feasible method for dye removal, but it produces a large amount of sludge, which in turn creates a disposal problem. Membrane processes require high pressure, and pores may be obstructed easily by suspended solids. Oxidation is a rapid process, but it uses chemical reagents to promote activation. It may also increase operational costs, thereby decreasing economic feasibility (Crini 2006). Among these methods, adsorption gives the best results as it can be applied to remove different types of dyes and produce high-quality treated effluent (Jain *et al*. 2003; Crini 2006). Rafatullah *et al.* (2010) even mentioned that adsorption was superior to other techniques for water re-use because of low initial cost, flexibility, simplicity of design, ease of operation, insensitivity to toxic pollutants, and no formation of harmful substances during application. Among all kinds of adsorbents, activated carbon is the most effective and the most widely used (Walker and Weatherley 1998). However, it is expensive and its regeneration by a refractory technique results in a 10 to 15% adsorbent loss, as well as a reduction of its adsorption capacity (Waranusantigul *et al.* 2003). Therefore, low-cost alternative adsorbents have been investigated as substitutes for activated carbon; these include abundant natural materials such as wood (Sahu *et al.* 2010; Khezami *et al.* 2007), coal (Liu *et al.* 2009), and agricultural wastes such as plum kernels (Tseng 2007), olive bagasse (Demiral *et al.* 2011), oil palm shell (Jia and Lua 2008), almond shells (Rodriguez-Reinoso *et al.* 1982), as well as industrial wastes such as tire rubber (Miguel *et al.* 2003), sewage sludge (Martin *et al.* 2002; Monsalvo *et al.* 2011), waste polyethylene terephthalate (PET) bottles (Nakagawa *et al.* 2004), fly ash (Mohan *et al.* 2002; Purnomo *et al.* 2012), and lignin (Hayashi *et al.* 2000). Importantly, for low-cost adsorbents, the manufacturing process should be as simple as possible to reduce the cost of production. Most of the references presented on this topic used activation processes to enhance the adsorption

capacity of adsorbents; however, activation processes increase costs because they require somewhat expensive equipment or chemical reagents. Such processes also require further treatment of derived corrosive gas (H_2SO_4) or Zn-containing solutions ($ZnCl_2$).

Paper sludge is a major waste by-product of the paper industry in Taiwan, and it contains water, fiber, organic compounds, inorganic salts, and mineral fillers (Maschio *et al.* 2009). It is believed that paper sludge can also be a precursor of carbonaceous adsorbents because of high organic content. In order to simplify the manufacturing process, paper sludge was pyrolyzed at 600°C for 1 h (thereafter refer to as P600) and washed with 1M HCl to become a carbonized adsorbent PC600. Both cationic (Methylene Blue, MB) and anionic (Procion Red MX-5B, PR) dyes were chosen as adsorbates in order to study the adsorption ability of PC600. Isotherm adsorption and adsorption kinetics experiments were also conducted, and Langmuir, Freundlich, and pseudo-first-order and pseudo-second-order equations were used to examine the experimental results. The maximum adsorption capacity and activated energy of adsorption were obtained, and the adsorption behavior of adsorbent derived from paper sludge toward ionic dyes was also evaluated.

EXPERIMENTS

Characteristics of Paper Sludge

The paper sludge utilized in this study came from a paper mill of eastern Taiwan. To understand the characteristics of the sludge, a sample was dried at 110°C and was analyzed using atomic absorption spectrometry (AAS, Varian, AA240), X-ray diffract-tometer (XRD, Rigaku), and ignition loss testing.

Chemical analysis was performed with 0.2 g of the sample mixed with 16 mL of aqua regia and 8 mL of hydrofluoric acid; this mixture was heated at 180°C for 3 h. The filtrate was diluted and analyzed using AAS. An X-ray diffractometer was used to examine and scan the crystalline phases of the dry sample from 10^o to 80^o (2θ) at a scan rate of 4 degrees per minute with a voltage and a current of 30 KV and 50 mA, respectively. For ignition-loss testing, 5 g of paper sludge (W_1) were heated at 800°C for 3 h. The weight of the ignited residue (W_2) was recorded while the sample cooled. The result of ignition loss was calculated according to Equation (1):

$$\textit{Loss on ignition}\ (\%) = \frac{W_1 - W_2}{W_1} \times 100\% \quad (1)$$

The Production and Characteristics of Adsorbent Derived from Paper Sludge

Dried paper sludge was placed in a crucible and heated with a tube furnace. The heating rate was 20^oC/min and the nitrogen flow was 2 L/min for 5 min in advance of heating. The carbonization process was carried out at 600°C for 1 h; the resultant residual was labeled as P600. After cooling, the carbonized solid sample was mixed with 1M HCl solution (40:1 liquid to solid ratio) for 30 min. After the acid treatment, the residual was twice washed with DI water. Finally, the sample was dried at 105°C and named PC600.

X-ray diffraction (XDF) analysis, specific surface area, and zeta potential were tested to understand the characteristics of the PC600. The XRD analysis procedure was

the same as that of sludge analysis. The specific surface area was measured from the N_2 adsorption isotherms at 77 K (-196°C) with an adsorption apparatus (Autosorb-1, Quantachrome) and calculated utilizing the BET (Brunauer-Emmet-Teller) method (Brunauer et al. 1938). Pore size distribution was calculated using the BJH (Barrett-Joyner-Halenda) method (Barrett et al. 1951). Approximately 0.1 g of PC600 was mixed with 1000 mL of 0.001M NaCl solution to determine the zeta potential of the adsorbents by a zeta potential analyzer (Nano Z, Malvern). The particles were dispersed in an ultrasonic cleaner for 30 min, and 1M HCl or NaOH solution was used to adjust the pH within a range of 2 to 10.

Adsorption Experiment

MB and PR were chosen as adsorbates; they were cationic and anionic dyes in aqueous solution, respectively. The adsorption of dyes was studied in batch mode, and the concentration of each sample determined by UV/Vis spectrometry (Lambda 25, Perkin Elmer) at wavelengths of 664 nm for MB and 538 nm for PR. The methods used for adsorption behavior are explained in the following subsections.

Effect of pH on adsorption

Approximately 0.25 g of PC600 was added into 25 mL of dye solution, of which the initial concentrations of dye were 1200 mg/L for MB and 500 mg/L for PR. The adsorption experiments were conducted at 30°C for 2 h. After the adsorption experiments, the solution was filtered, and the concentrations of MB and PR were determined using UV/Vis spectrometry.

Chemical oxygen demand (COD) was also measured for the filtrates after adsorption according to the standard method of the National Institute of Environmental Analysis (NIEA W5.17.52B) of Taiwan. Approximately 2.5 mL of filtrate, 1.5 mL of 0.02 M $K_2Cr_2O_7$, and 3 mL of Ag_2SO_4/H_2SO_4 solution were mixed and heated at 150°C for 2 hrs. After cooling, the solution was titrated with 0.25 M $(NH_4)_2Fe(SO_4)_2$; ferroin (1,10-phenanthroline monohydrate, $C_{12}H_8N_2 \cdot H_2O$) was used as an indicator. A blank sample was prepared by substituting 2.5 mL of the filtrate for 2.5 mL of DI water. When the color of the solution changed from yellow to red, the end point of titration was reached. The value of COD obtained from Equation (2),

$$COD\ (mg/L) = \frac{(A-B)\times M \times 8000}{V} \quad (2)$$

where A and B were the volume (mL) of $(NH_4)_2Fe(SO_4)_2$ consumption in the blank and sample, respectively; M was the concentration of $(NH_4)_2Fe(SO_4)_2$ (mol/L); and V was the volume (mL) of DI water or filtrate.

Isotherm adsorption

The time of equilibrium adsorption was determined before isotherm adsorption. The initial dye concentration was the same as that mentioned above, and the ratio of adsorbent versus dye solution was 0.25 g/25 mL. The adsorption tests were carried out at 30°C from 5 min to 6 h to determine the equilibration time.

Isotherm adsorption experiments were conducted for different initial concentrations (1200, 1500, 1800, and 2100 mg/L for MB, and 500, 750, 1000, and 1250

mg/L for PR). The adsorbent concentration and adsorption temperature were the same as those above, but the adsorption time was 4 h. After adsorption, the experimental results were examined using Langmuir (Eq. (3)) and Freundlich (Eq. (4)) isotherm models:

$$\frac{C_e}{Q_e} = \frac{C_e}{Q_m} + \frac{1}{Q_m K_L} \quad (3)$$

$$\log Q_e = \log K_F + \frac{1}{n} \log C_e \quad (4)$$

where C_e is the dye concentration in solution at equilibrium; Q_e is the adsorption capacity of the adsorbent at equilibrium; Q_m is the maximum capacity of the adsorbent; and K_L is the Langmuir adsorption constant (L/mg). The term K_F is the Freundlich constant (L/mg), and n is the heterogeneity factor for the Freundlich isotherm model.

Kinetic adsorption

The results of the kinetics study were obtained for different temperatures (30, 45, and 60°C) and adsorption times (10, 20, 40, 60, and 80 min.). The ratio of adsorbent versus dye solution was 0.25 g/ 25 mL, and the initial concentrations of MB and PR were 1200 and 500 mg/L, respectively. The results were analyzed with two adsorption kinetic models, namely, the pseudo-first-order (Eq. (5)) and pseudo-second-order kinetic models (Eq. (6)):

$$\log(Q_e - Q_t) = \log Q_e - \frac{k_1}{2.303} t \quad (5)$$

$$\frac{t}{Q_t} = \frac{1}{k_2 Q_e^2} + \frac{1}{Q_e} t \quad (6)$$

where Q_e (mg/g) is the adsorption capacity at equilibrium, and Q_t (mg/g) is the adsorption uptake at time t (min.). The terms k_1 and k_2 are the rate constants of the pseudo-first-order and pseudo-second-order models.

RESULTS AND DISCUSSION

Characteristics of paper sludge and PC600

The results of chemical and ignition loss analyses of the paper sludge used in this study are shown in Table 1. The water content was 65%, and the ignition loss of the dry sludge was 54.68%. High values of ignition loss indicated the high organic content of the paper sludge. After ignition loss test, the paper sludge ash was digested with aqua regia and hydrofluoric acid. The element concentration of ash was determined by AAS. The compositions are presented as oxides, and the values are listed in Table 1. The major inorganic element of paper sludge was Ca, which might arise from the neutralizer used in wastewater treatment (*i.e.* lime or slaked lime) or papermaking filler used in the papermaking process (Ochoa de Alda 2008). Silicon content took second place. The percentage of SiO_2 in paper sludge was 16.7 %. Other elements present in the paper sludge such as Mg, Al, Na, and K were not abundant and the percentages of these oxides

were all less than 2 %. The result of the XRD analysis (see Fig. 1) matched the chemical analysis and showed that the major component of the sludge was $CaCO_3$.

Table 1. Analysis of Paper Sludge

	Water content (%)	CaO	SiO_2	MgO	Al_2O_3	Na_2O	K_2O	Loss on Ignition (%)
Paper sludge	65.0	20.90	16.70	1.81	1.26	1.22	0.38	54.68
P600	--	30.94	16.35	6.08	1.56	3.44	0.35	41.79
PC600	--	0.27	35.33	2.87	3.7	4.42	0.91	52.27

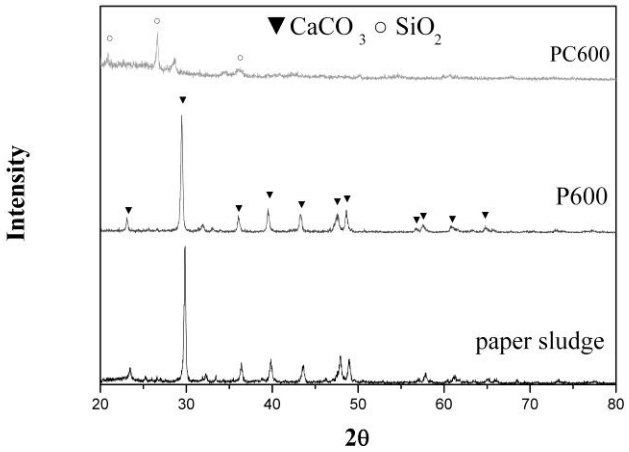

Fig. 1. XRD analysis of the paper sludge, P600 and PC600. P600 was pyrolyzed paper sludge without acid washing. PC600 was pyrolyzed paper sludge with acid washing.

After pyrolysis, according to the XRD analysis in Fig. 1, $CaCO_3$ was still the principal crystal phase of the P600, since the decomposition temperature of $CaCO_3$ is higher than 700°C (Yang *et al.* 2008) and the pyrolysis temperature used in this study was below the decomposition temperature of $CaCO_3$. P600 was then washed with 1M HCl and DI water to form PC600. Acid washing was applied for two reasons: one is that paper sludge is an alkaline waste and the pH value of dye solution would have increased during the adsorption experiment. The reason for this was probably the amount of acidic surface functional groups decreasing in the organic fraction and the surface of the sample becoming more alkaline during pyrolysis (Rio *et al.* 2006). Another possible reason is inorganic salt (such as calcium carbonate in the adsorbent) being removed, leading to an increase in the specific surface area of the adsorbent, which led to improved adsorption ability. After acid washing, the major crystal phase of PC600 changed to SiO_2 because of the dissolution of calcium carbonate. Ros *et al.* (2006) investigated pyrolyzed sewage sludge washed with 5 M HCl. The ash content dropped from 66.1% to 45.5%, and the specific surface area increased from 13 m^2/g to 188 m^2/g. Chemical analyses revealed that the Fe, Ca, and Mg contents decreased and the weight percent of Si increased. Bagreev *et al.* (2001) also investigated sewage sludge pyrolysis and reported that the specific surface area increased from 17 m^2/g to 41 m^2/g after acid washing with 16% HCl. In this study, the loss on ignition of PC600 was 52.27%, which was higher than that of P600 in Table 1. In addition, the CaO and MgO contents decreased from 30.94% to 0.27% and 6.08% to 2.87%, and the content of insoluble ingredients such as SiO_2 and

Al_2O_3 increased from 16.35% to 35.33% and 1.56% to 3.7%, respectively. The results corresponded to the XRD analysis, and most of the Ca salts were dissolved by HCl. SEM images also showed the effects of acid washing on calcium salt dissolution.

Figure 2 gives SEM images of P600 and PC600, and reveals that particle size was obviously reduced with acid washing treatment. Corresponding to the results of SEM imaging, specific surface area increased from 13.25 to 193.86 m^2/g after acid washing. The adsorption capacities of MB for P600 and PC600 were 29.38 and 115.7 mg/g, respectively and those for PR were 19.15 and 51.6 mg/g, respectively. Adsorption conditions were 30°C for 4 h (the initial concentrations of MB and PR were 1200 mg/L and 500 mg/L, respectively). The results show that acid washing can increase adsorption capacity by increasing specific surface area.

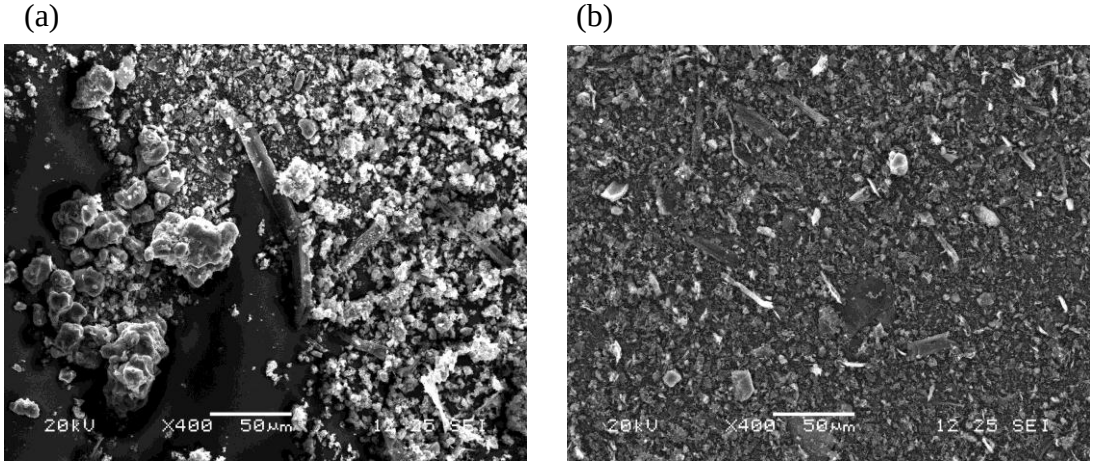

Fig. 2. SEM images of P600 and PC600 (x400): (a) P600 (b) PC600.

PC600 was chosen as dye adsorbent. The specific surface area was 193.86 m^2/g, and most of the pore diameter (by volume) was between 2.5 to 5 nm, according to the BJH method (see Fig. 3); this data suggested that PC600 was a mesoporous adsorbent. The pore volume can also be calculated from the amount of N_2 adsorbed at different P/P_0 condition (Hayashi *et al.* 2000), where P and P_0 were the partial pressure and saturated vapor pressure of N_2, respectively. The volume of the micropore was calculated from the amount of adsorption at $P/P_0 = 0.1$. The value corresponding to $P/P_0 = 0.1$ was 0.0714 cm^3/g. On the other hand, the volume of the total pore was 0.1870 cm^3/g, which was calculated at $P/P_0 = 0.95$. The volume of the mesopore was obtained by subtracting the micropore volume from total pore volume (*i.e.* 0.1156 cm^3/g). The ratio of the volume of the micropores to the total pore volume was 38.18%, whereas the mesopores was 61.82%. These results indicated that the mesopores were a major constituent of PC600.

The zeta potential of the PC600 was also measured to evaluate the surface charge of PC600. The results are shown in Fig. 4. The zeta potential was affected by the pH conditions. The zeta potential value was positive in acidic and negative in alkaline conditions. The isoelectric point of PC600 was around pH 3, which indicated that the zeta potential was 0 at ~pH 3. Zeta potential can afford electrostatic attraction or repulsion of ions, which was important consideration for ionic dye adsorption in this study.

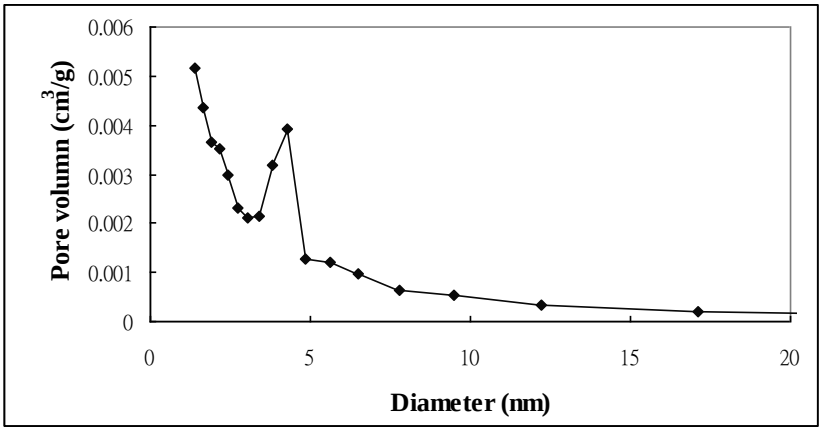

Fig. 3. Pore volume distribution of PC600

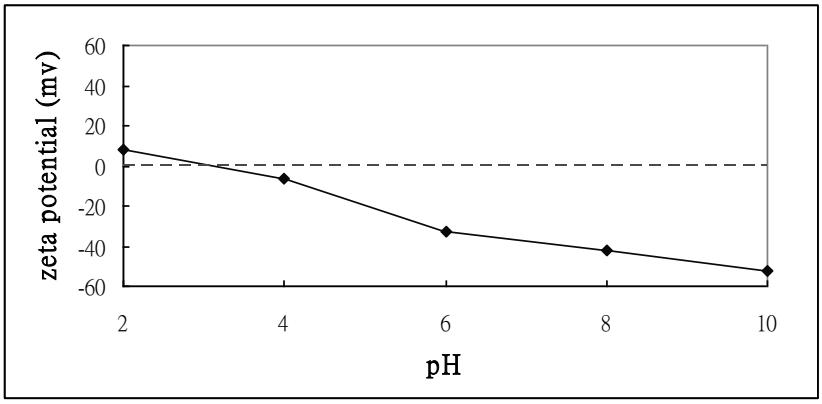

Fig. 4. Zeta potential of the PC600 from pH 2 to pH 10

Adsorption Experiment

Effect of pH on dye adsorption

Adsorption pH conditions are an important variable for dye adsorption. Cationic dyes tend to be adsorbed at relatively high pH values, whereas anionic dyes are generally adsorbed at low pH (Hubbe *et al.* 2012). The results of ionic dye adsorption by PC600 are shown in Fig. 5. The adsorption of MB increased but PR decreased with increased pH. The phenomenon can be ascribed to the zeta potential of PC600, which was positively charged at low pH conditions and attracted anion dyes such as PR. By contrast, the cationic dye of MB was adsorbed well at high pH conditions where the zeta potential was negative. Besides, electrostatic attraction was not the only adsorption mechanism due to the adsorption of MB at pH 2.6 and that of PR at pH 7.5. In these situations, PC600 possessed the same charge as ionic dyes, but the adsorption percentage of MB and PR were still higher than 50%. This cannot be explained by electrostatic interaction. The adsorption of organic compounds, aromatic compounds in particular, involves a complex interplay of electrostatic and dispersive interactions (Rivera-Utrilla and Sánchez-Polo 2002). Ayranci and Duman (2006) reported that the cationic state of nicotinic acid and 4-aminobenzoic acid can be adsorbed by activated carbon, for which the surface was definitely positively charged in 0.4M H_2SO_4 solution. On the other hand, benzoic acid,

nicotinic acid, and 4-aminobenzoic acid were monoanonic in 0.1 M NaOH solution and adsorbed in small amounts on activated carbon even though the surface charge of activated carbon was negative. The authors mentioned that the dispersion interactions and either the π-electrons of the aromatic ring or the dipole of adsorbates overcame the electrostatic repulsion, thereby assisting the adsorption process. In our study, MB and PR were also aromatic compounds; thus the adsorptions of MB in acid solution and of PR in alkali solution might also be assisted by dispersion interactions.

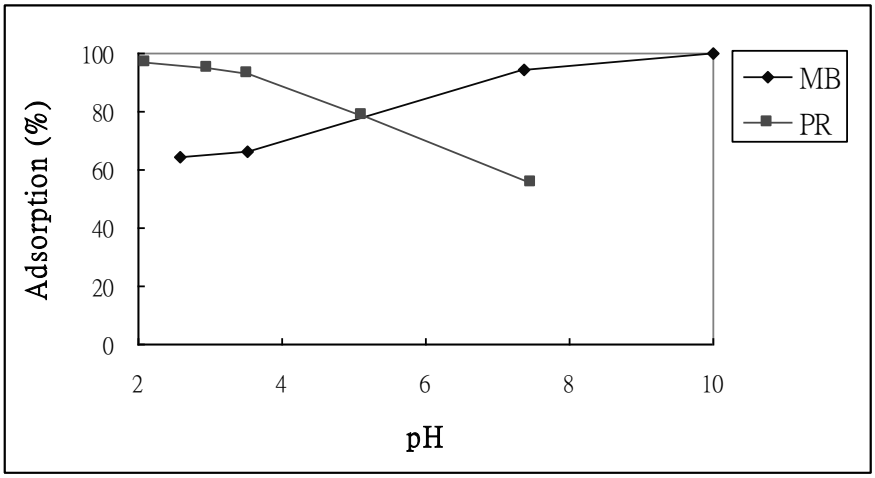

Fig. 5. Adsorption of MB and PR at different pH conditions. (MB initial concentration: 1200 mg/L; PR initial concentration: 500 mg/L, adsorption condition: 30 ^{o}C, 4 h)

Chemical oxygen demand (COD) was also used to measure the adsorption efficiency of PC600. COD is one of the wastewater effluent parameters monitored and regulated by Taiwan. COD indicates the organic pollution load in water and is defined as the number of oxygen equivalents consumed in the oxidation of organic compounds using strong oxidizing agents, such as $K_2Cr_2O_7$ (Yang *et al.* 2011). The results are shown in Fig. 6.

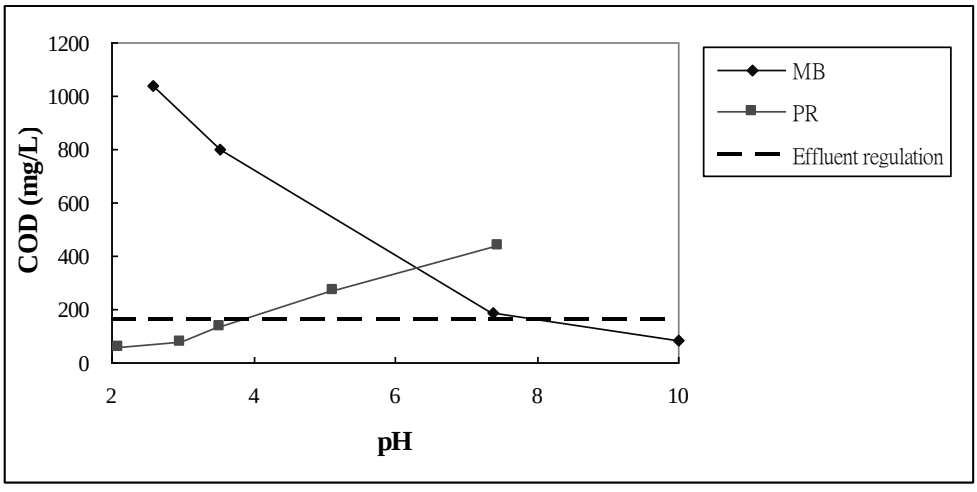

Fig. 6. Chemical oxygen demand (COD) of the filtrate of MB and PR adsorption for different pH conditions

The dashed line shows the effluent standards for Taiwan at 160 mg/L. The COD value of the filtrate correlated with the residual concentration of dye, which was high at a low adsorption percentage. For MB adsorption, the residual concentration in pH 7.5 was 74.6 mg/L and the COD value was 184 mg/L. On the other hand, the residual concentration and the COD value for PR in pH 3.5 were 35.4 mg/L and 136 mg/L, respectively. In other words, the residual concentrations should be lower than 74.6 mg/L for MB and 35.4 mg/L for PR to ensure the values of COD are lower than the regulatory requirement.

Isotherm adsorption

Adsorption equilibrium time was measured in the first step, and the adsorption conditions are listed: at pH = 7.5, 1200 mg/L of the MB initial dye concentration and at pH = 3.5, 500 mg/L of the PR initial dye concentration. The ratio of PC600 versus dye solution was 0.25 g/25 mL for both dyes and adsorption temperature was 30°C. The results are shown in Fig. 7. The adsorption percentages increased quickly over the 30 min. for both MB and PR adsorptions. Equilibrium time was considered to be 4 h for PC600.

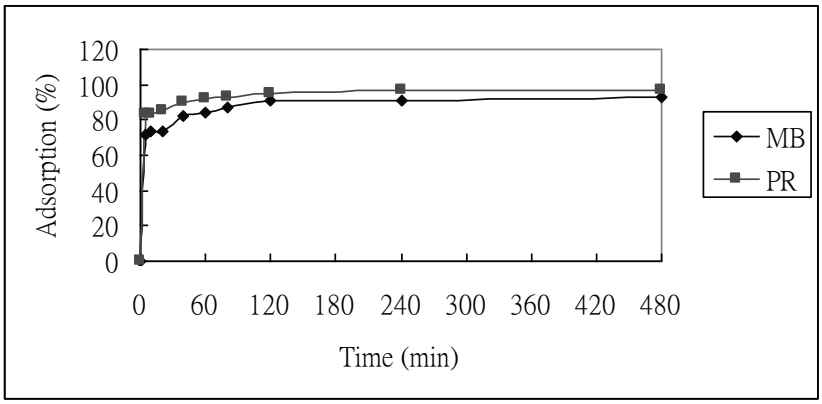

Fig. 7. Dye adsorption percentage versus time

Isotherm adsorption experiments were conducted for different initial concentrations (1200, 1500, 1800, and 2100 mg/L for MB, and 500, 750, 1000, and 1250 mg/L for PR), and the results are listed in Table 2. The results were modeled using Langmuir (Eq. (3)) and Freundlich (Eq. (4)) equations. The coefficients of determination (R^2) for the equation fittings and the parameter values for each equation are listed in Table 3. For the Langmuir equation, the values of Q_m and K_L were from the slope and intercept of the linear plots of C_e/Q_e versus C_e, and the values of n and K_F were from the slope and intercept of the linear plots of log Q_e versus log C_e for the Freundlich equation. The R^2 value of Langmuir was higher than that of Freundlich, which means the adsorption behaviors of MB and PR fit the Langmuir better than Freundlich model. The Freundlich adsorption isotherm is a relationship between the amount of adsorption and the concentration of the adsorbate in the liquid. This is an empirical equation and may fail to fit the experiment data at high adsorbate concentrations. Maximum adsorption capacity can be calculated from the Langmuir equation. The value for MB was 119.04 mg/g and that for PR was 65.79 mg/g. The values of the adsorption capacity show that PC600 possessed higher adsorption ability toward MB than PR.

Table 2. Isotherm Adsorption Results of PC600

Dye	Initial Concentration (mg/L)	C_e (mg/L)	Q_e (mg/g)
MB	1200	114.5	115.7
	1500	350.6	116.0
	1800	660.4	116.5
	2100	970.5	118.6
PR	500	15.0	51.6
	750	185.8	55.1
	1000	386.4	60.6
	1250	610.5	65.02

Table 3. Parameters of Adsorption Isotherm Models Fitting for MB and PR

Dye	Langmuir				Freundlich		
	Q_m(mg/g)	K_L(L/mg)	R^2	R_L	n	K_F	R^2
MB	119.04	0.14	0.9998	0.0034-0.0059	104.17	110.2	0.6311
PR	65.79	0.05	0.9958	0.016-0.038	17.79	43.5	0.8318

The dimensionless separation factor, R_L, was calculated from the fitted Langmuir isotherm equation to determine the type of adsorption process (Tseng, 2007),

$$R_L = \frac{1}{1 + K_L C_i} \quad (7)$$

where C_i is the initial concentration of the adsorption process and R_L is classified as: $R_L > 1$ meaning unfavorable adsorption; $0 < R_L < 1$, meaning favorable adsorption; and $R_L = 0$, meaning irreversible adsorption (Tseng, 2007). In this study, the R_L value of MB and PR was between 0 to 1 when C_i was between 1200 to 2100 mg/L for MB, and 500 to 1250 mg/L for PR. The R_L value indicates that the adsorption types for MB and PR were favorable when PC600 was utilized.

Adsorption kinetics

Adsorption kinetics can be analyzed using of pseudo-first-order and pseudo-second-order kinetic models (Lin *et al.* 2011). Hubbe *et al.* (2012) mentioned that the adsorption which fitted pseudo-first-order model might be correlated to certain functional groups on the substrates. On the contrary, the adsorption kinetics fitted with pseudo-second-order model probably represented that the rate-determining step of adsorption involved two functional groups at the substrate surface. Besides, the adsorption rate was depended on the square of the unfilled adsorption sites since the origin form of Eq. 6 was:

$$\frac{dQ_t}{dt} = k_2 \left(Q_e - Q_t\right)^2 \quad (8)$$

The fact that the adsorption behavior corresponds to the pseudo-second-equation should reveal that the last remaining sites become increasingly reluctant to be filled. In this study, the adsorption temperatures were 30, 45, and 60°C, and the adsorption durations were 10, 20, 40, 60, and 80 min. The initial concentrations for MB and PR were 1200 mg/L and 500 mg/L, respectively. As a result, a higher R^2 value represents the adsorption kinetics of MB and PR fitting well with the pseudo-second-order kinetic

model (see Table 4). The adsorption of ionic dye was not correlated to certain functional groups but was affected by both electrostatic and dispersion interaction. The two interactions might affect the rate-determining step of adsorption, and the correlation coefficient of *t/Qt* versus *t* was close to 1 when the pseudo-second-order model was utilized.

The temperature dependence of rate constants can be described by the Arrhenius equation:

$$\ln k_2 = \ln A - \frac{E_a}{RT} \quad (9)$$

where k_2, A, E_a, R, and T represent the rate constant, frequency factor, activation energy, gas constant, and absolute temperature of the pseudo-second-order model. The value of activation energy (E_a) can be obtained by the slope of plotting ln k_2 against 1/T. The values of E_a for MB and PR adsorption were 12.32 and 2.88 kJ/mol, respectively. Additionally, the magnitude of E_a can provide clues if the adsorption process is chemical or physical process (Han *et al.* 2009). Values of E_a for physical adsorption are usually < 4.2 kJ/mol since the forces involved in physical adsorption are weak. Chemical adsorption involves forces much stronger than in physical adsorption and the values of E_a are typically between 8.4 and 83.7 kJ/mol. Non-activated chemical adsorption has E_a values near zero (Aksu 2002). In this study, according to the E_a values, the adsorption types of PR and MB should be physical and activated chemical adsorption, respectively.

Table 4. Parameters of Adsorption Kinetics Models Fitting for MB and PR

Dye	Temperature (°C)	R^2		K_2 (g/mg/min)	E_a (kJ/mol)
		1st order	2nd order		
MB	30	0.8928	0.9997	0.002026	12.32
	45	0.8751	0.9995	0.002421	
	60	0.8095	0.9993	0.003154	
PR	30	0.9178	0.9998	0.011751	2.88
	45	0.7336	0.9997	0.012461	
	60	0.7558	0.9996	0.013023	

CONCLUSIONS

Paper sludge was pyrolyzed at 600°C for 1 h and washed with 1M HCl to form carbonaceous adsorbent (PC600) for MB and PR. PC600 was a found to be mesoporous material having a specific surface area of 193.86 m^2/g and a pore diameter distribution of 2.5 to 5 nm. The isoelectric point was located at pH 3, meaning that the particles of PC600 possessed a positive charge at pH < 3 and negative charge at pH > 3. The adsorption results of MB and PR fitted the Langmuir equation well, and the maximum adsorption capacities of MB and PR were 119.04 mg/g and 65.79 mg/g, respectively. The COD value of the filtrate after MB adsorption in pH 10 was 81.6 mg/L, and that of PR in pH 3 was 78 mg/L. These values are lower than the 160 mg/L requirement for effluent standards in Taiwan. The adsorption behavior of both dyes fitted the pseudo-second-order kinetic model, and the respective activation energies calculated from the Arrhenius

equation for MB and PR were 12.32 and 2.88 kJ/mol. Accordingly, the adsorption types of MB and PR should be classed as chemical and physical adsorption, respectively.

REFERENCES CITED

Aksu, Z. (2002). "Determination of the equilibrium, kinetic and thermodynamic parameters of the batch biosorption of nickel (II) ions onto *Chlorella vulgaris*," *Process Biochem.* 38(1), 89-99.

Ayranci, E., and Duman, O. (2006). "Adsorption of aromatic organic acids onto high area activated carbon cloth in relation to wastewater purification," *J. Hazard. Mater.* 136(3), 542-552.

Bagreev, A., Bandosz, T. J., and Locke, D. C. (2001). "Pore structure and surface chemistry of adsorbents obtained by pyrolysis of sewage sludge-derived fertilizer," *Carbon* 39(13), 1971-1979.

Barrett, E.P., Joyner, L.G., Halenda, P.P. (1951). "The determination of pore volume and area distributions in porous substances. 1. Computations from nitrogen isotherms," *J. Am. Chem. Soc.* 73(1), 373-380.

Brunauer, S., Emmett, P.H., Teller, E. (1938). "Adsorption of gases in multimolecular layers," *J. Am. Chem. Soc.* 60(2), 309-319.

Crini, G. (2006). "Non-conventional low-cost adsorbents for dye removal: A review," *Bioresource Technol.* 97(9), 1061-1085.

Doğan, D., and Türkdemir, H. (2005). "Electrochemical oxidation of textile dye indigo," *J. Chem. Technol. Biotechnol.* 80(8), 916-923.

Demiral, H., Demiral, I., Karabacakoğlu, B., and Tümsek, F. (2011). "Production of activated carbon from olive bagasse by physical activation," *Chem. Eng. Res. Des.* 89(2), 206-213.

Gupta, V. K., and Suhas. (2009). "Application of low-cost adsorbents for dye removal – A review," *J. Environ. Manage.* 90(8), 2313-2342.

Han, R., Zhang, J., Han, P., Wang, Y., Zhao, Z., and Tang, M. (2009). "Study of equilibrium, kinetic and thermodynamic parameters about methylene blue adsorption onto natural zeolite," *Chem. Eng. J.* 145(3), 496-504.

Hayashi, J., Kazehaya, A., Muroyama, K., and Watkinson, A. P. (2000). "Preparation of activated carbon from lignin by chemical activation," *Carbon* 38(13), 1873-1878.

Hubbe, M. A., Beck, K. R., O'Neal, W. G., Sharma, Y. Ch. (2012). "Cellulosic substrates for removal of pollutants from aqueous systems: A review. 2. Dyes," *BioResources* 7(2), 2592-2687.

Jain, A. K., Gupta, V. K., Bhatnagar, A., and Suhas. (2003). "Utilization of industrial waste products as adsorbents for the removal of dyes," *Journal of Hazardous Materials* B101, 31-42.

Jia, Q., and Lua, A. C. (2008). "Effects of pyrolysis conditions on the physical characteristics of oil-palm-shell activated carbons used in aqueous phase phenol adsorption," *J. Anal. Appl. Pyrol.* 83(2), 175-179.

Khezami, L., Ould-Dris, A., and Capart, R. (2007). "Activated carbon from thermo-compressed wood and other lignocellulosic precursors," *BioResources* 2(2), 193-209.

Kim, T. H., Park, C., and Kim, S. (2005). "Water recycling from desalination and purification process of reactive dye manufacturing industry by combined membrane filtration," *J. Clean. Prod.* 13(8), 779-786.

Lin, Y. F., Chen, H. W., Chien, P. S., Chiou, C. S., and Liu, C. C. (2011). "Application of bifunctional magnetic adsorbent to adsorb metal cations and anionic dyes in aqueous solution," *J. Hazard. Mater.* 185(2-3), 1124-1130.

Liu, Z., Zhou, A., Wang, G., and Zhao, X. (2009). "Adsorption behavior of methyl orange onto modified ultrafine coal powder," *Chinese J. Chem. Eng.* 17(6), 942-948.

Lucas, M. S., and Peres, J. A. (2006). "Decolorization of the azo dye Reactive Black 5 by Fenton and photo-Fenton oxidation," *Dyes Pigments.* 71(3), 236-244.

Martin, M. J., Artola, A., Balaguer, M. D., and Rigola, M. (2002). "Towards waste minimization in WWTP: Activated carbon from biological sludge and its application in liquid phase adsorption," *J. Chem. Technol. Biot.* 77(7), 825-833

Maschio, S., Furlani, E., Tonello, G., Faraone, N., Aneggi, E., Minichelli, D., Fedrizzi, L., Bachiorrini, A., and Bruckner, S. (2009). "Fast firing of tiles containing paper mill sludge, glass cullet and clay," *Waste Manage.* 29(11), 2880-2885.

Miguel, G. S., Fowler, G. D., and Sollars, C. J. (2003). "A study of the characteristics of activated carbons produced by steam and carbon dioxide activation of waste tyre rubber," *Carbon* 41(5), 1009-1016.

Mohan, D., Singh, K. P., Singh, G., and Kumar, K. (2002). "Removal of dyes from wastewater using flyash, a low-cost adsorbent," *Ind. Eng. Chem. Res.* 41(15), 3688-3695.

Monsalvo, V. M., Mohedano, A. F., and Rodriguez, J. J. (2011). "Activated carbons from sewage sludge. Application to aqueous-phase adsorption of 4-chlorophenol," *Desalination* 277(1-3), 377-382.

Nakagawa, K., Namba, A., Mukai, S. R., Tamon, H., Ariyadejwanich, P., and Tanthapanichakoon, W. (2004). "Adsorption of phenol and reactive dye from aqueous solution on activated carbons derived from solid wastes," *Water Res.* 38(7), 1791-1798.

Ochoa de Alda, J. A. G. (2008). "Feasibility of recycling pulp and paper mill sludge in the paper and board industries," *Resources, Conservation and Recycling* 52(7), 965-972.

Olivella, M. À., Fiol, N., Torre, F. D. L., Poch, J., and Villaescusa I. (2012). "A mechanistic approach to methylene blue sorption on two vegetable wastes: Cork bark and grape stalks," *BioResources.* 7(3), 3340-3354.

Purnomo, C. W., Salim, C., and Hinode, H. (2012). "Effect of the activation method on the properties and adsorption behavior of bagasse fly ash-based activated carbon," *Fuel Process. Technol.* 102(October 2012), 132-139.

Rafatullah, M., Sulaiman, O., Hashim, R., Ahmad, A. (2010) "Adsorption of methylene blue on low-cost adsorbents: A review," *Journal of Hazardous Materials,* 177, 70-80.

Rio, S., Le Coq, L., Faur, C., Lecomte, D., and Le Cloirec, P. (2006) "Preparation of adsorbents from sewage sludge by steam activation for industrial emission treatment," *Process Safty and Environmental Protection,* 84(B4), 258-264.

Rivera-Utrilla, J., and Sánchez-Polo, M. (2002). "The role of dispersive and electrostatic interactions in the aqueous phase adsorption of naphthalenesulphonic acids on ozone-treated activated carbons," *Carbon,* 40(14), 2685-2691.

Rodriguez-Reinoso, F., Lopez-Gonzalez, J. de D., and Berenguer, C. (1982). "Activated carbons from almond shells-1: Preparation and characterization by nitrogen adsorption," *Carbon* 20(6), 513-518.

Ros, A., Lillo-Ródenas, M. A., Fuente, E., Montes-Morán, M. A., Martin, M. J., and Linares-Solano, A. (2006). "High surface area materials prepared from sewage sludge-based precursors," *Chemosphere.* 65(1), 132-140.

Sahu, J. N., Acharya, J., and Meikap, B. C. (2010). "Optimization of production conditions for activated carbons from Tamarind wood by zinc chloride using response surface methodology," *Bioresource Technol.* 101(6), 1974-1982.

Shi, B. Y., Li, G. H., Wang, D. S., Feng, C. H., and Tang, H. X. (2007a). "Removal of direct dyes by coagulation: The performance of preformed polymeric aluminum species," *J. Hazard. Mater.* 143(1-2), 567-574.

Shi, B. Y., Li, G., Wang, D., and Tang, H. (2007b). "Separation of Al_{13} from polyaluminum chloride bisulfate precipitation and nitrate metathesis," *Sep. Purif. Technol.* 54(1), 88-95.

Sun, Q., and Yang, L. (2003). "The adsorption of basic dyes from aqueous solution on modified peat-resin particle," *Water Res.* 37(7), 1535-1544.

Tseng, R. L. (2007). "Physical and chemical properties and adsorption type of activated carbon prepared from plum kernels by NaOH activation," *J. Hazard. Mater.* 147(3), 1020-1027.

Walker, G. M., and Weatherley, L. R. (1998). "Fixed bed adsorption of acid dyes onto activated carbon," *Environ. Pollut.* 99(1), 133-136.

Waranusantigul, P., Pokethitiyook, P., Kruatrachue, M., and Upatham, E. S. (2003). "Kinetics of basic dye (methylene blue) biosorption by giant duckweed (*Spirodela polyrrhiza*)," *Environ. Pollut.* 125(3), 385-392.

Yang, D. H., Hur, B. Y., and Yang, S. R. (2008). "Study on fabrication and foaming mechanism of Mg foam using $CaCO_3$ as blowing agent," *J. Alloy Compd.* 461(1-2), 221-227.

Yang, J., Chen, J., Zhou, Y., and Wu, K. (2011). "A nano-copper electrochemical sensor for sensitive detection of chemical oxygen demand," *Sensor Actuat. B: Chem.* 153(1), 78-82.

Article submitted: October 20, 2012; Peer review completed: December 8, 2012; Revised version received and accepted: January 7, 2013; Published: January 9, 2013.